

---

This is an electronic reprint of the original article.  
This reprint may differ from the original in pagination and typographic detail.

Brooshan, Elmira; Kauppila, Tommi; Szlachta, Małgorzata; Jooshaki, Mohammad; Leveinen, Jussi

## Utilizing Recycled concrete aggregate for treating Acid mine drainage

*Published in:*  
Cleaner Materials

*DOI:*  
[10.1016/j.clema.2023.100205](https://doi.org/10.1016/j.clema.2023.100205)

Published: 01/09/2023

*Document Version*  
Publisher's PDF, also known as Version of record

*Published under the following license:*  
CC BY-NC-ND

*Please cite the original version:*  
Brooshan, E., Kauppila, T., Szlachta, M., Jooshaki, M., & Leveinen, J. (2023). Utilizing Recycled concrete aggregate for treating Acid mine drainage. *Cleaner Materials*, 9, Article 100205.  
<https://doi.org/10.1016/j.clema.2023.100205>

---

This material is protected by copyright and other intellectual property rights, and duplication or sale of all or part of any of the repository collections is not permitted, except that material may be duplicated by you for your research use or educational purposes in electronic or print form. You must obtain permission for any other use. Electronic or print copies may not be offered, whether for sale or otherwise to anyone who is not an authorised user.



## Utilizing Recycled concrete aggregate for treating Acid mine drainage

Elmira Brooshan<sup>a,\*</sup>, Tommi Kauppila<sup>b</sup>, Małgorzata Szlachta<sup>b,c</sup>, Mohammad Jooshaki<sup>d</sup>,  
Jussi Leveinen<sup>f</sup>

<sup>a</sup> Water Management Solutions (VER) Unit, Geological Survey of Finland, Espoo 02151, Finland

<sup>b</sup> Circular Economy Solutions (KTR) Unit, Geological Survey of Finland, Kuopio 70211, Finland

<sup>c</sup> Faculty of Environmental Engineering, Wrocław University of Science and Technology, Wybrzeże Wyspiańskiego 27, 50-370 Wrocław, Poland

<sup>d</sup> Circular Economy Solutions (KTR) Unit, Geological Survey of Finland, Kokkola 67100, Finland

<sup>f</sup> Department of Civil Engineering, Aalto University, Espoo 02150, Finland

### ARTICLE INFO

#### Keywords:

Recycled concrete aggregate  
Acid mine drainage  
Mine water treatment  
Sulfate  
Heavy metal removal  
Sustainability

### ABSTRACT

This study focuses on treating Acid Mine Drainage (AMD) using Recycled Concrete Aggregate (RCA) as a cost-effective and environmentally friendly material. RCA is utilized, considering its availability at low cost, to reduce heavy metal and sulfate concentration in AMD and neutralize its acidity in batch experimental mode. To that end, the adsorptive properties of RCA were characterized before and after adsorption by Scanning Electron Microscopy (SEM), Energy Dispersive Spectroscopy (EDS), elemental mapping, Brunauer-Emmett-Teller (BET) surface area measurements, and X-ray Diffraction. Furthermore, the organic functional groups of the tested materials were identified by Fourier Transform Infrared Spectroscopy (FT-IR). Adsorption parameters such as dosage, contact time, the grain size distribution of adsorbent particles, and the solution pH, were optimized for enhancing the removal performance. The pH point of zero charges for the RCA sample was defined. The results revealed that RCA is a potential eco-friendly material for AMD treatment. The concentration of sulfate in the tested AMD water was reduced by approximately 84%, while that of the metal elements declined as follows: iron 100%, manganese 95%, copper 66%, zinc 97%, and lead 76%. Also, the pH value of AMD water increased rapidly and reached neutral by using small quantities of RCA ( $\leq 1$ g/L).

### 1. Introduction

Aside from the natural phenomena, anthropogenic activities, including mining industries, are the major producers of acid sulfur-rich waters (Johnson & Hallberg, 2005). Mining activities are among the most significant sources of Acid Mine Drainage (AMD) pollution, which is classified as a serious environmental concern (Macías et al., 2017). AMD contains high volumes of hazardous trace elements and sulfur-compounds besides the low pH (Komnitsas et al., 2004). The high concentration of heavy metals and sulfate can cause severe effects on soil, water resources, aquatic ecosystems, as well as human health (WHO, 2008, 2011; Shim et al., 2015; Galhardi & Bonotto, 2016; Kefeni et al., 2017).

Typically, AMD can occur in many active, closed, and abandoned mines. However, abandoned or closed mines in countries with a long history of mining are at higher risk of generating toxic water (Younger et al., 2002; Carrero et al., 2015; Fernando et al., 2018). The characteristics of AMD depend on the composition and mineralogy of the

mined ore and country rocks and minerals being extracted and processed (Szlachta et al., 2020). Especially those mines that extracted sulfide ores can produce acidity for several years, even decades, if not managed properly (Arroyo & Siebe, 2007). As the characteristics of AMD are highly variable, monitoring and predicting the reactions of AMD in the environment can be challenging and costly (Baruah & Khare, 2010; Grande et al., 2010; Aguiar et al., 2016; Qureshi et al., 2016; Kefeni et al., 2017). Thus, a low-maintenance water treatment method for AMD using low-cost materials is highly required.

Current research and industry interests are focused on the environmental and sustainable applications of low-cost adsorptive materials for water treatment (Ali & Gupta, 2007; Lin & Juang, 2009; Mohan & Gandhimathi, 2009; Rafatullah et al., 2010; Wang et al., 2010; Keng et al., 2014; Lakherwal, 2014; Lim & Aris, 2014; Kumara et al., 2017; Panda et al., 2020). Nowadays, using lime and limestone is a common approach for treating AMD water in the mining industry (Potgieter-Vermaak et al., 2006). Limestone contains a high amount of calcium carbonate, which can bind sulfate ions and neutralize mine water

\* Corresponding author.

E-mail address: [elmira.brooshan@gtk.fi](mailto:elmira.brooshan@gtk.fi) (E. Brooshan).

(Hammack et al., 1994; Silva et al., 2012). Very fine limestone contains 95% calcium carbonate (Oates, 1998).

In recent years, urbanization development has produced a massive amount of RCA due to demolishing of concrete structures. Construction and demolition waste constitutes approximately 30% of total waste produced globally (Purchase et al. 2022) with an estimated 35% ending directly in landfills (Menegaki & Damigos 2018). While coarse RCA can be used in new concrete, fine RCA still presents unresolved challenges for reuse in construction due to lack of data on its properties and performance of the final products (Nedeljković et al., 2021). Additionally, the improper disposal of concrete waste can lead to environmental issues such as air and water pollution (Pallewatta et al., 2023).

Due to the limitations in using fine RCA in the construction sector, a use as an added-value product for water treatment can be considered as an environmentally responsible and economically viable alternative. Due to its high surface area and alkaline properties, RCA has the potential to be used as an adsorbent for mine water treatment. However, there is a scarcity of knowledge on the use of RCA as a cost-effective sustainable adsorbent to treat acidic mine water. Recycled construction aggregate contains high amounts of adsorptive minerals. While different minerals have been studied for treating AMD, RCA remains unexplored for such an environmentally friendly purpose. Some recent literature suggested that concrete fines can be used as an effective and environmentally friendly alternative for AMD treatment. The neutralization performance, sedimentation performance, and CO<sub>2</sub> emissions-related considerations were found to be satisfactory (Ho et al., 2023; Iizuka et al., 2022).

Aijala is a closed sulfide mine site located in the southwest of Finland. With a high concentration of sulfate and trace metals in waters, Aijala was selected as an appropriate case for the studies in this research (Kokkola, 1982; Isomäki, 1990; Sipilä, 1994; Valjus et al., 2017). We collected water samples from Aijala tailings area, identified by field measurements as acidic with high conductivity, suggesting high dissolved concentrations of possible trace metals in the water. Initial analyses on the water samples revealed high concentrations of sulfate and metals such as zinc (Zn), iron (Fe), copper (Cu), manganese (Mn), and lead (Pb). [Supplementary Information](#).

The primary objective of this research was to determine the effect of RCA treatment on the concentration of sulfate, iron, zinc, copper, manganese, and lead in the heavily polluted mine water. Thus, neutralizing AMD, buffering its acidity, and removing the main pollutants through adsorption processes were the main research goals.

To accomplish the goals, first the characteristics of the RCA adsorbent were determined before and after adsorption testing by several characterization methods. Brunauer-Emmett-Teller (BET) measurement was used to measure the surface area and porosity of the adsorbent. Scanning Electron Microscopy (SEM), Energy Dispersive Spectroscopy (EDS), and X-ray Diffraction (XRD) analyses were employed to identify the elemental and mineral compositions, surface morphology, and the crystallinity of the adsorbent. Fourier Transform Infrared Spectroscopy (FT-IR) was used to study the reactions of the contaminants at the surface of the adsorbent. Adsorption batch experiments were conducted in order to examine the effectiveness of the removal of sulfate and heavy metals using RCA as adsorbent. The effects of process parameters such as adsorbent dosage, pH, adsorbent particle size, and the contact time were investigated.

Accordingly, this research introduces the potential of treating AMD with RCA as an effective, low-cost, and sustainable method. As a passive method of mine water treatment by RCA, this approach considers the principles of sustainability, cost-effectiveness, and environmental friendliness. The detailed aims of the study are 1) characterize the properties of RCA as an adsorbent, 2) conduct experiments of using RCA as an adsorbent to remove sulfate from AMD, 3) metals removal, and 4) study the changes in the RCA material after treatment of AMD.

**Table 1**

Aijala water quality measurement results in the field dated May 17, 2019.

Tailing area	Date	Temperature (°C)	pH	O <sub>2</sub> (mg/L)	Conductivity (µS/cm)
Aijala	17.05.2019	19.6	4.16	5.09	1794

**Table 2**

The initial concentration of the targeted elements.

Element	SO <sub>4</sub> <sup>2-</sup>	Pb	Mn	Fe	Cu	Zn
Aijala water (mg/l)	1035.60	0.07	0.59	0.33	0.05	2.71

## 2. Materials and methods

Herein, the adsorptive behavior of sulfate and heavy metals dissolved in the AMD onto RCA was assessed. Mine water samples for testing were collected from Aijala tailings pond. [Table 1](#) shows the initial water quality parameters in the field from the targeted areas. Also, [Table 2](#) represents the initial concentration of the targeted elements. As can be inferred from the results, Aijala AMD water is highly polluted and requires treatment. It is worth mentioning that all the chemicals used were laboratory-grade provided by Merck, USA. Materials were prepared daily before the experiment, including pH adjustment.

### 2.1. Preparation of adsorbent

RCA was obtained from a construction materials company for testing as a cost-effective and sustainable adsorbent for mine water treatment. Rudus Company provided the RCA with particle size between 0 and 45 mm for this study. The crushed concrete was mainly made of hollow core concrete with an average concrete strength of C50 and stress class of XC1. The material was a mixture of several qualities as a whole (Rudus, 2019).

Initially, the RCA material was heated in a drying oven at 90 °C for 24 h to remove the moisture content, followed by cooling to room temperature for 8 h. The material was cooled in the Nalgene™-S317-0180, Acrylic Desiccator Cabinets-USA. All the heating and drying steps were done with the laboratory incubator from BINDER GmbH, Tuttlingen, Germany, model-BD23.

The RCA sample was homogenized and sieved to different particle sizes as smaller than 80 µm, 80 µm-200 µm, 200 µm-630 µm, 630 µm-2 mm, 2 mm-6.3 mm, and larger than 6.3 mm and smaller than 45 mm. Retsch GmbH, Germany, equipment was used for the sieving process as shown in [Fig. 1](#). In this figure, (a) shows the RCA mixture as received from the supplier, while (b) and (c) respectively illustrate the sieves and six different sieved particle sizes. All the above RCA sizes were assessed to explore the optimal grain size of the adsorbent for maximum removal.

### 2.2. Characterization of the adsorbent

The RCA was characterized by BET, which measures the physical adsorption of nitrogen gas on a solid surface. The specific surface area was determined using the nitrogen gas adsorption method within the 0.01–0.1 relative pressure range at –195.86 °C. Reference measurements were conducted on a BELsorp Mini II specific surface area and pore size measuring unit (MicrotracBEL Corp, Japan). The pore size distribution was performed using the Dollimore-Heal (DH) method to determine pore radii.

Scanning Electron Microscopy/Energy Dispersive Spectroscopy (SEM-EDS) and elemental mapping were conducted with an analytical high-resolution JEOL JSM-7500FA-USA scanning electron microscope. Due to the non-conductivity of the RCA material, a coating process was required to facilitate observation and high resolution in SEM. To prepare

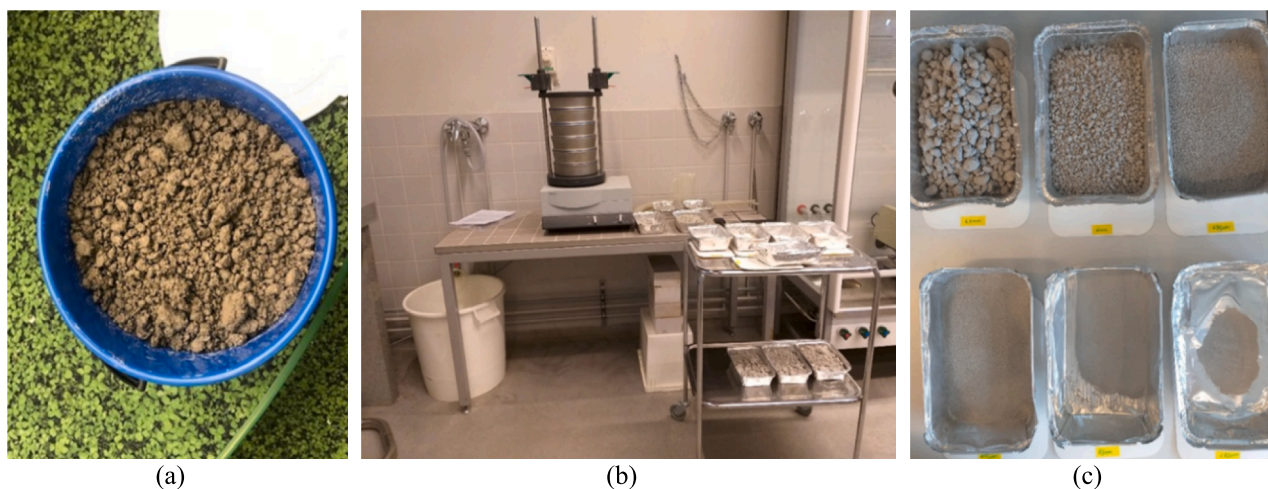


**Fig. 1.** The sieving process of the recycled concrete aggregates with the sieve sizes of 80  $\mu\text{m}$ , 80  $\mu\text{m}$ -200  $\mu\text{m}$ , 200  $\mu\text{m}$ -630  $\mu\text{m}$ , 630  $\mu\text{m}$ -2 mm, 2 mm-6.3 mm, and larger than 6.3 mm and smaller than 45 mm; (a) initial RCA mixture; (b) sieving apparatus; (c) sieved fractions.

the sample, a thin layer of RCA was placed on the sample holder by carbon tape. A Leica EM ACE600 sputter coater-USA was used to coat a 5.16 nm layer of Gold Palladium (Au-Pd) on the sample. The resolution limiting factor was the grain size, which was 5F20 nm depending on the sputtering conditions. A uniform layer without noticeable grains was produced on the sample surface. EDS was utilized for elemental mapping of the RCA before and after treatment to identify the elements influenced in the sample after the sorption tests.

The samples were analyzed on an X-ray Diffraction (XRD) instrument, Malvern Panalytical CubiX3, UK, equipped with cobalt (Co) X-ray tube. XRD is a fast analytical technique used for phase identification of crystalline materials.

Organic functional groups were identified by Fourier Transform Infrared Spectroscopy (FT-IR). The samples were measured with Perkin Elmer/ Labsence, USA, Model: spectrum Two Polymer QA/QC Analysis System. FT-IR spectra of the samples were measured within the range of 400–4000  $\text{cm}^{-1}$ . An extra set of measurements was performed on the solid content of the water samples before and after adsorption. To prepare the solid content, water samples before and after adsorption were boiled to remove the water and collect the remaining solid substrate. The collected solids were then analyzed by FT-IR.

### 2.3. Point of zero charge (PZC)

The batch equilibrium method was applied to examine the point of zero charges (PZC) of the RCA at room temperature ( $23 \pm 2$   $^{\circ}\text{C}$ ). First, 5.844 g of NaCl (molar mass 58.44 g/mol) was dissolved in one liter of deionized (DI) water. Subsequently, the initial pH in the NaCl solution was adjusted from 2 to 12 for the tests. The adjustments were done by using 0.1 M HCl or 0.1 M NaOH. To study the isoelectric point of RCA, 2 g of RCA (particle size < 80  $\mu\text{m}$ ) was added to 25 mL of solution with a pH ranging from 2 to 12. The mixtures were kept for 24 h at room temperature ( $23 \pm 2$   $^{\circ}\text{C}$ ). The final pH was measured two times for all samples and the average was recorded.

**Table 3**  
Characteristics of the surface of the adsorbents.

Adsorbent	Pore size (nm)	Specific surface area ( $\text{m}^2/\text{g}$ )	Pore volume ( $\text{cm}^3/\text{g}$ )
Before sulfate adsorption	36.45	10.96	0.0999
After sulfate adsorption	29.71	14.77	0.1097

### 2.4. Adsorption experiments

Comparing the amount of sulfate and heavy metals in the water samples revealed higher concentration of sulfate. Hence, sulfate removal was studied first, followed by tests of the removal of heavy metals.

For sulfate removal testing, batch adsorption experiments were conducted by mixing mine water samples and a known amount of RCA at room temperature ( $23 \pm 2$   $^{\circ}\text{C}$ ) and at 210 rpm agitation speed on a shaker. The pH values were adjusted by using 0.1 M HCl or 0.1 M NaOH solution. The initial experiments were carried out on Aijala AMD water to test the sulfate adsorption performance of the RCA. As sulfate is anionic, the pH value was adjusted to 2 daily before the experiment. After adsorption experiments, the treated water was filtered through a filter with a pore size of 0.45  $\mu\text{m}$  from Sartorius Company, Germany, model nisart with a sterile syringe.

To examine the pH effect on sulfate adsorption, the pH value of Aijala AMD water was adjusted to 2, 4, 6, and 12. The mixtures were mixed for 72 h containing 150 g/L of the finest size (<80  $\mu\text{m}$ ) of RCA. The final pH values were also measured for each set.

To study the effect of adsorbent dosage on sulfate removal, the Aijala water samples adjusted at pH 2 were mixed with RCA in the range of 50, 75, 100, 125, 150, 200, and 250 g/L. The pH adjustment was done as the highest sulfate removal was achieved at this pH value and AMD waters are typically acidic. After finding the optimal adsorbent dosage, this mixture was shaken from 6 h to 96 h to study the optimal contact time. To explore the effect of particle size, several particle sizes of RCA classified by sieving were applied using the optimized RCA dosage and contact time from previous sets.

A similar process of testing was used for investigating metal removal while considering that metals are cationic, pH adjustment was not required. It was observed that iron removal requires a smaller amount of the adsorbent than sulfate or the other metals. Therefore, iron removal tests were conducted by mixing 0.05, 0.10, 0.15, 0.20, 0.25, 0.50, 1.00, and 5.00 g/L into AMD Aijala water in constant contact time of 24 h with the finest size (<80  $\mu\text{m}$ ) of RCA.

All the adsorption experiments were repeated three times at room temperature ( $23 \pm 2$   $^{\circ}\text{C}$ ). The adsorption was calculated using Equation (1), where  $R$  is adsorption (%),  $C_0$  (mg/L) represents initial concentration of adsorbate, and  $C_e$  (mg/L) is the equilibrium concentration of ion (Iakovleva et al., 2015).

$$R = \left( \frac{C_0 - C_e}{C_0} \right) * 100 \quad (1)$$

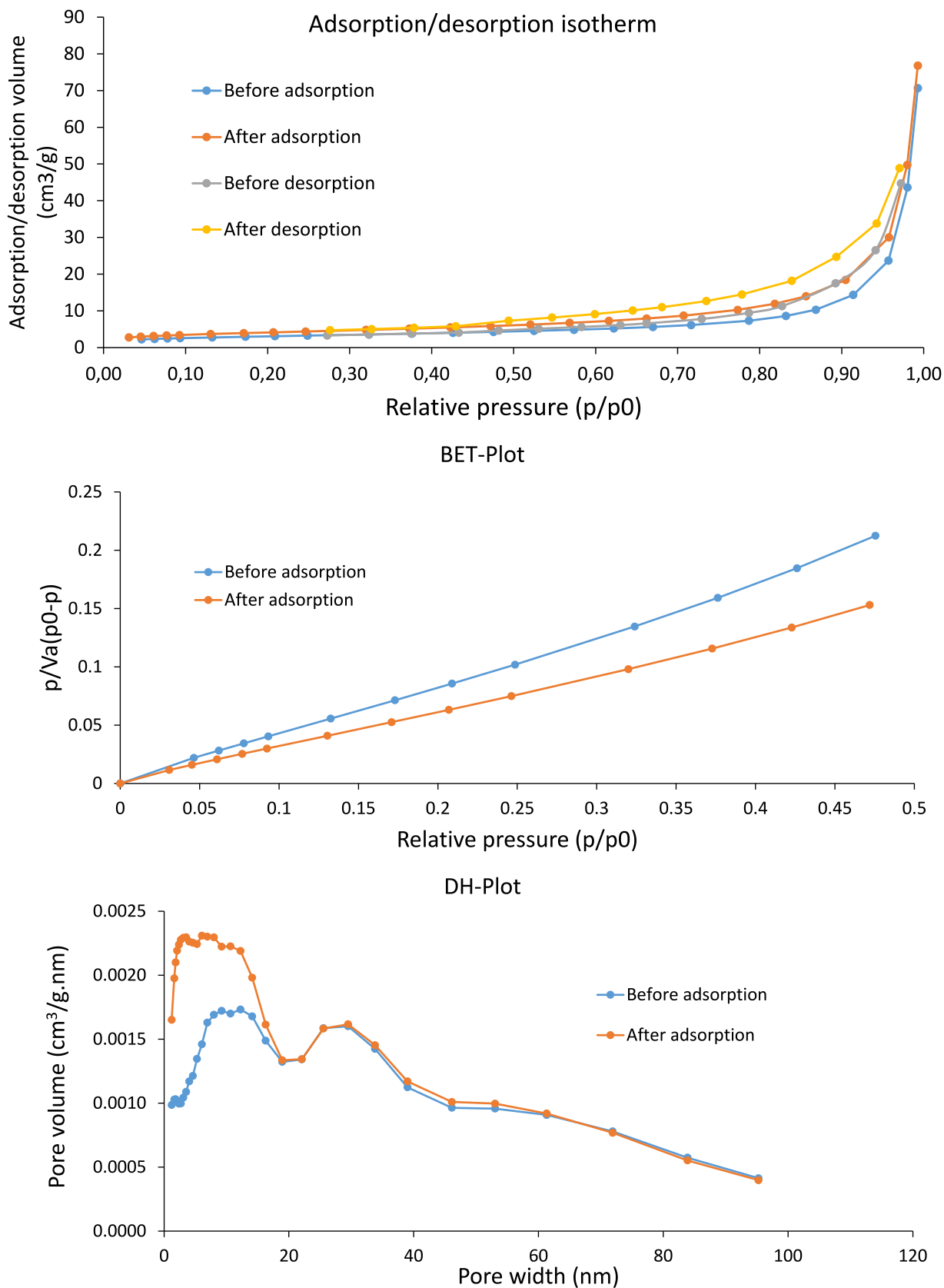
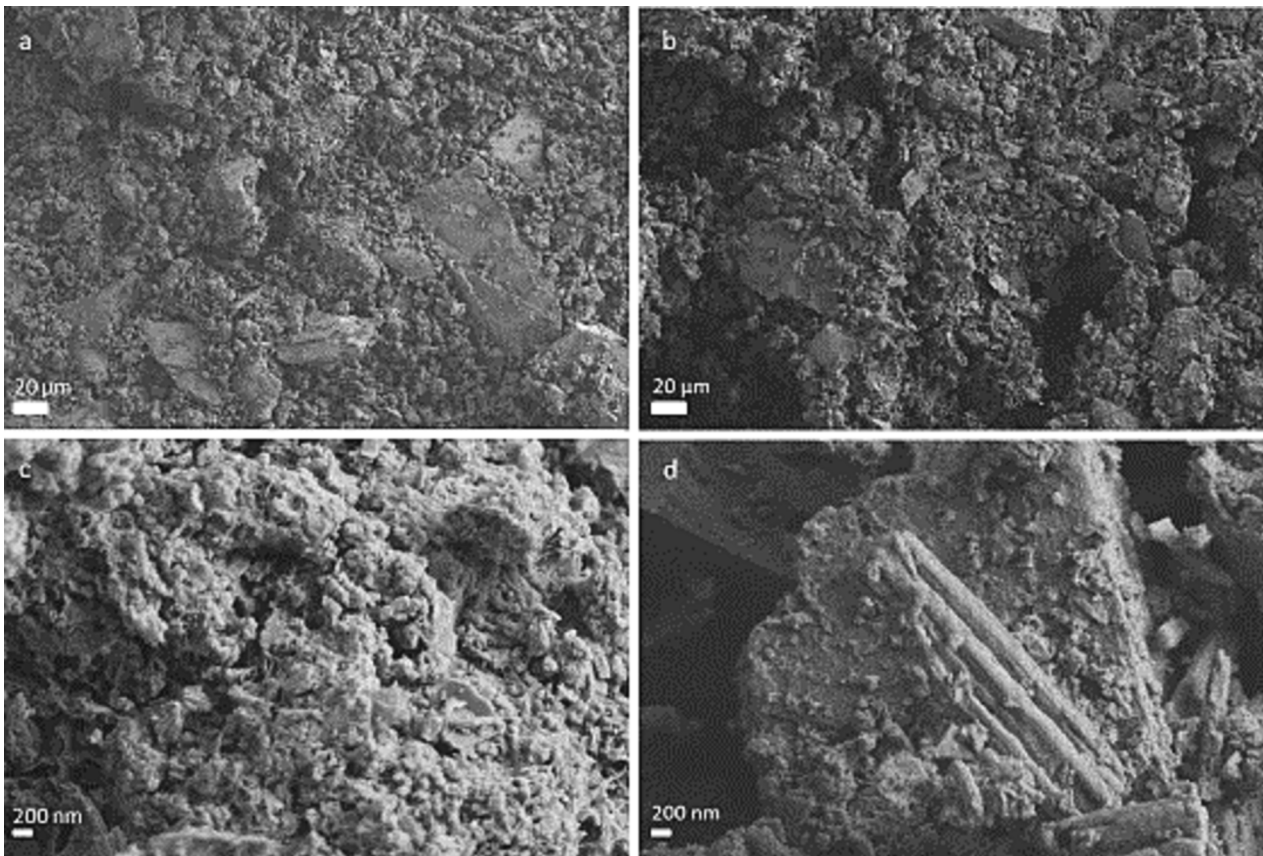
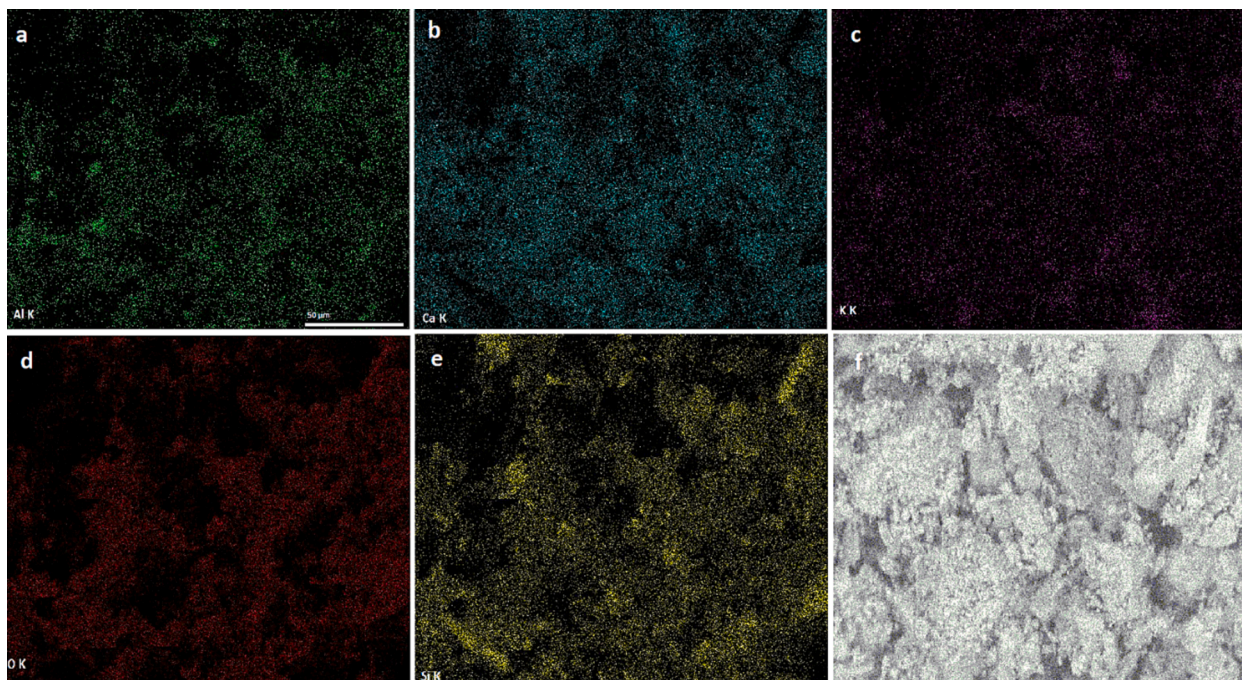


Fig. 2. Adsorption/desorption isotherm, Brunauer-Emmett-Teller (BET), and Dollimore-Heal (DH) measurements for RCA material before and after sulfate adsorption. The measurements were done with N<sub>2</sub> at temperature 77 K and saturated vapor pressure (p<sub>0</sub>) 100.80 kPa. Where p is the pressure of the adsorptive; p/p<sub>0</sub> is the relative pressure; V<sub>a</sub> is the volume of nitrogen adsorbed per gram of solid.



**Fig. 3.** SEM images of RCA before sulfate adsorption (a) and after sulfate adsorption (b) in micro scale; and SEM measurements of RCA before sulfate adsorption (c) and after sulfate adsorption (d) in nanoscale.



**Fig. 4.** SEM image of RCA material before sulfate adsorption with element distributions maps of a) Al, b) Ca, c) K, d) O, e) Si, and f) the surface image of the area.

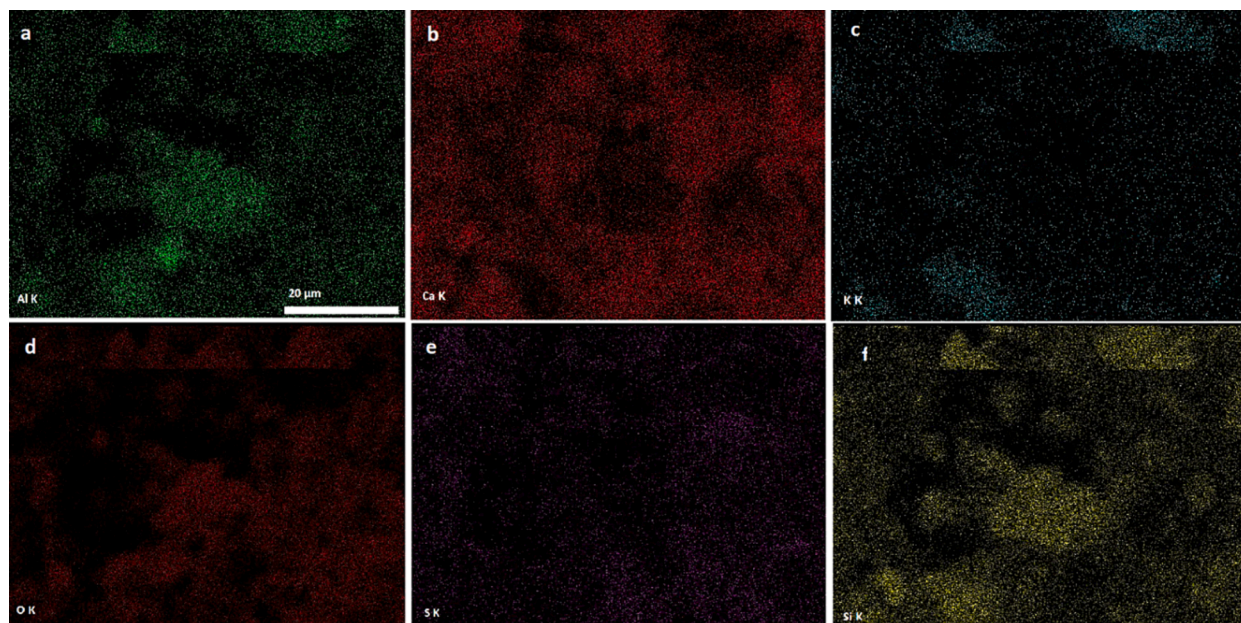


Fig. 5. SEM image of RCA material after sulfate adsorption with element distributions maps of a) Al, b) Ca, c) K, d) O, e) S, and f) Si.

### 3. Results and discussion

#### 3.1. Changes in the characteristics of the adsorbent in the tests before and after treatment

Surface area and porosity are among the influential characteristics of an adsorbent. A higher surface area and porosity result in higher adsorption due to providing more adsorptive sites for the accommodation of the adsorbate (Yazdani et al., 2019). Table 3 and Fig. 2 show the adsorption–desorption curves with BET and porosity via Dollimore-Heal

(DH) for material before and after water treatment. The specific surface area was measured as 11 m<sup>2</sup>/g before and 14.8 m<sup>2</sup>/g after adsorption. The pore size distribution of the RCA mainly ranged between 1 and 100 nm, with an average size of 36.5 nm for the raw sample and 29.7 nm for the sample after the process. Comparing the material before and after water treatment shows that the specific surface area and total pore volume are increased, and the mean pore size is reduced. This might stem from precipitation of metal oxides and calcium sulfate on the surface of the solid leading to a higher porosity and surface area especially due to an increase in very small pores (0–20 nm, Fig. 2). This

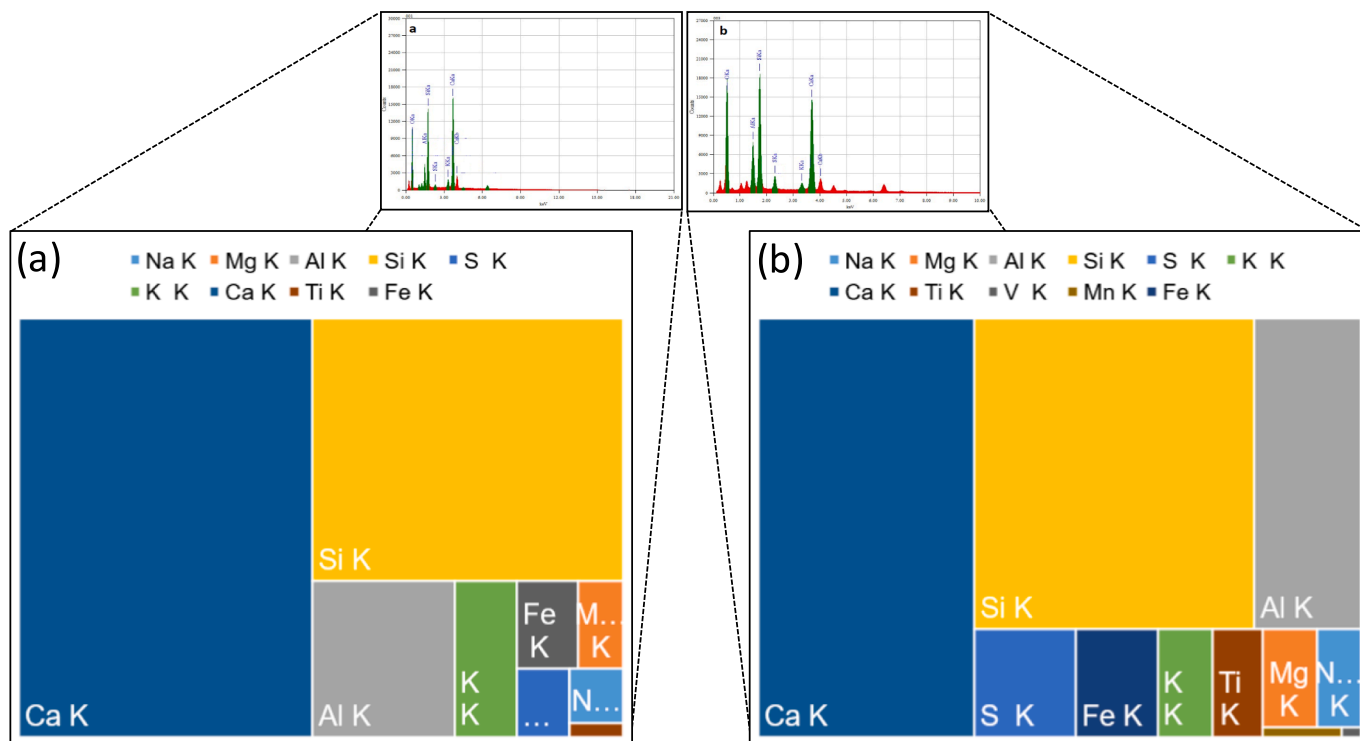


Fig. 6. Energy Dispersive Spectra (EDS) and corresponding element counts proportional-area graphs for RCA (a) before sulfate adsorption, and (b) after sulfate adsorption (Higher-resolution EDS are available in Figures S11 and S12 of the supplementary material).

**Table 4**

Elemental composition of RCA surface in mass (%), and Mol (%) before and after sulfate adsorption; higher values in bold font (Detailed data in Tables SI1 and SI2 of the supplementary material).

Element	Before adsorption		After adsorption	
	Mass%	Oxide Mol%	Mass%	Oxide Mol%
O	37.49	–	<b>39.98</b>	–
Na	0.48	0.63	<b>0.70</b>	<b>0.97</b>
Mg	0.63	1.58	<b>0.83</b>	<b>2.18</b>
Al	3.77	4.25	<b>5.49</b>	<b>6.46</b>
Si	14.23	30.86	<b>14.83</b>	<b>33.54</b>
S	0.78	1.49	<b>2.35</b>	<b>4.66</b>
K	<b>2.66</b>	<b>2.07</b>	1.59	1.29
Ca	<b>36.10</b>	<b>54.86</b>	25.96	41.15
Ti	0.29	0.37	<b>2.08</b>	<b>2.76</b>
Fe	3.55	3.87	<b>5.70</b>	<b>6.48</b>
Mn	–	–	<b>0.41</b>	<b>0.48</b>
V	–	–	<b>0.08</b>	<b>0.05</b>
<b>Total</b>	100	100	100	100

porosity would thus be secondary in nature, caused by the materials adsorbed or precipitated onto the RCA, rather than a change in the properties of the RCA itself.

SEM, a type of electron microscope, produces images with a focused beam of electrons by scanning the surfaces of solid objects for instant studies. SEM images presented in Fig. 3 compare classification of particles in the surface area of the adsorbent before and after water treatment in nano and micro scales. As per Fig. 3 (a), the original material contains euhedral and subhedral crystals of aggregate, whereas Fig. 3 (b) shows an increase in the amount of subhedral crystals and anhedral material after water treatment which indicates that adsorption or precipitation happened in the process (Roedder, 1959). According to Fig. 3, before adsorption images, i.e., a and c, show the rough and porous surface of the adsorbent, which suggests that there was a high potential for the adsorption. Moreover, by imaging the surfaces of the particles after sulfate adsorption (Fig. 3. b and d), it is visually observed that the caves, pores, and surfaces of adsorbent were covered by a layer of adsorbed or precipitated pollutants.

Elemental mapping shows the distribution of elements within the sample. Elemental mapping before and after adsorption are presented in Fig. 4 and Fig. 5, respectively. These figures show that a large part of the RCA surface area was covered by Al, Ca, K, O, and Si containing particles before adsorption. EDS reveals the elemental analysis or chemical characterization of a sample. EDS spectra for the RCA material in Fig. 6 and Table 4, confirm the presence of major elements such as Ca, O, and Si. On the other hand, after the adsorption process, adsorbent adsorbs sulfate from the AMD water, as there is an increase in the mass of sulfur in the adsorbent. Data from EDS and elemental mapping prove that the adsorption process releases calcium and potassium. In contrast, based on Table 4, it consumes sulfur, oxygen, iron, and aluminum that are taken from polluted mine water generated by sulfuric ore bedrock. In addition to the mentioned ions, manganese and vanadium are also adsorbed by the adsorbent, although their mass percentages are negligible due to their small mass: 0.41% and 0.08%, respectively.

XRD method is used for characterizing crystalline structure of the material. Quartz, albite, and calcite peaks were identified from XRD patterns, shown in Fig. 7 for the RCA before and after adsorption. By comparing the XRD patterns before and after water treatment, it is observed that there is a reduction in the XRD patterns of quartz ( $\text{SiO}_2$ ) and albite ( $\text{NaAlSi}_3\text{O}_8$ ). In addition, portlandite and gypsum have been replaced by ettringite which is 3%.

Gypsum and sulfate compounds react with calcium aluminate in the cement to form ettringite. After adsorption, part of the sulfate is consumed to form ettringite indicating that formation of ettringite is one of the mechanisms removing sulfate from the mine water. The increase in calcite ( $\text{CaCO}_3$ ) is shown by carbonation, where  $\text{Ca}(\text{OH})_2$  is converted to calcium carbonate. Generally, calcite is found in the CaO and  $\text{SiO}_2$

system, when there is the presence of Al and  $\text{SO}_3$  (Pacheco-Torgal et al., 2015). Such an observation was also supported by the mineral mapping in Fig. 4 and Fig. 5, in addition to the EDS measurements in Fig. 6.

FT-IR is an analytical method to quickly and definitively identify organic, polymeric, inorganic materials. The FT-IR analysis method uses infrared light to scan samples and observe chemical properties. The FT-IR spectra were studied between 400 and 4000  $\text{cm}^{-1}$  for both the RCA before and after adsorption and the solid content of water sample, illustrated in Fig. 8 and Fig. 9, respectively. The FT-IR spectra for RCA adsorbent samples show several bands. The bands in 1360–1500  $\text{cm}^{-1}$  correspond to  $\text{C}=\text{C}-\text{H}$  and  $\text{C}=\text{C}$ . Moreover, the bands at 1000–1140  $\text{cm}^{-1}$ , and 480–500  $\text{cm}^{-1}$  correspond to sulfate compounds,  $\text{C}=\text{S}$  and  $-\text{S}-\text{S}-$ , respectively (Hase, 1999). Figs. 8 and 9 show Sulfur compounds have been removed, which proves sulfate removal from AMD water. In Fig. 9, there is a gap between two curves related to the sulfur compounds binding, Fig. 8 confirms adsorption happened. However, the FT-IR spectra for treated water clearly shows that the bands at 1000–1100  $\text{cm}^{-1}$  corresponding to sulfur compounds have been removed, demonstrating sulfate removal from AMD water. The band is 1000–1140  $\text{cm}^{-1}$  attributes to the band of  $\text{S}-\text{O}$  stretching (Socrates, 2002).

The pH of point zero charge (pH pzc) is commonly defined as the pH where the adsorbent surface provides a zero net charge (Bakatula et al., 2018). Solution pH is a crucial parameter in the sulfate adsorption process, as it could significantly impact the surface charge of the adsorbent and consequently the adsorption of the sulfate. The results from isoelectric measurement of RCA, which is illustrated in Fig. 10, indicates that the pH(pzc) is around 11 for the adsorbent (point of zero charge). Considering that the multivalent sulfate anions are adsorbed below the pH(pzc) due to the positive surface charge of the adsorbent, the acidic pH of the AMD can benefit the adsorption (Yazdani et al., 2016).

### 3.2. Characterization of the adsorbent surface sulfate removal tests

The dosage of the adsorbent plays a critical role in the adsorption process. Therefore, the effect of the adsorbent dosage on heavy metals and sulfate removal from AMD was studied. The correlation between dosage and sulfate removal is illustrated in Fig. 11. Accordingly, an increasing adsorption was observed by increasing dosage. Increased dosage provides more active sites and surface area for adsorption. Moreover, the correlation may result from the high concentration gradient between the pollutant and the adsorbent (Masukume et al., 2014). In addition, the adsorption process is also affected by the pH of the solution (see Fig. 14 below).

The highest removal (85%) was achieved at 150 g/L of adsorbent; hence, this dosage was selected as the optimal dosage for the rest of the sulfate experiments.

The variation of sulfate adsorption with contact time is plotted in Fig. 12, where increasing the contact time up to 72 h enhances sulfate removal (%). However, further increasing the contact time leads to a decrease in removal. As per Fig. 12, there is a significant rise in the adsorption while increasing the contact time from 6 to 12 hours, implying an initial stage with a high adsorption potential. This phenomenon commonly happens due to the high number of free active sites on the surface of the adsorbent. From 12 h up to 72 h there is a steady increase in adsorption (slower reaction rate stage). Further increase of time to 96 h causes a notable drop in the removal, which can be due to a release of adsorbed molecules back to the water (desorption). Besides, there might be a repulsion and excretion between the existing ions in the solution and those adsorbed on the surface area (Alley, 2007). The decrease in adsorption with the contact time increasing beyond 72 h may be related to the increase in the pH of the solution. In the 72 h experiments testing the effects of pH on the adsorption, the final pH of the solution typically reached pH 10–12 (Fig. 14) while the pH remained near 7 in the 24 h experiments (e.g., Figs. 15 and 16). The extended high pH conditions may explain the decrease in adsorption beyond 72 h

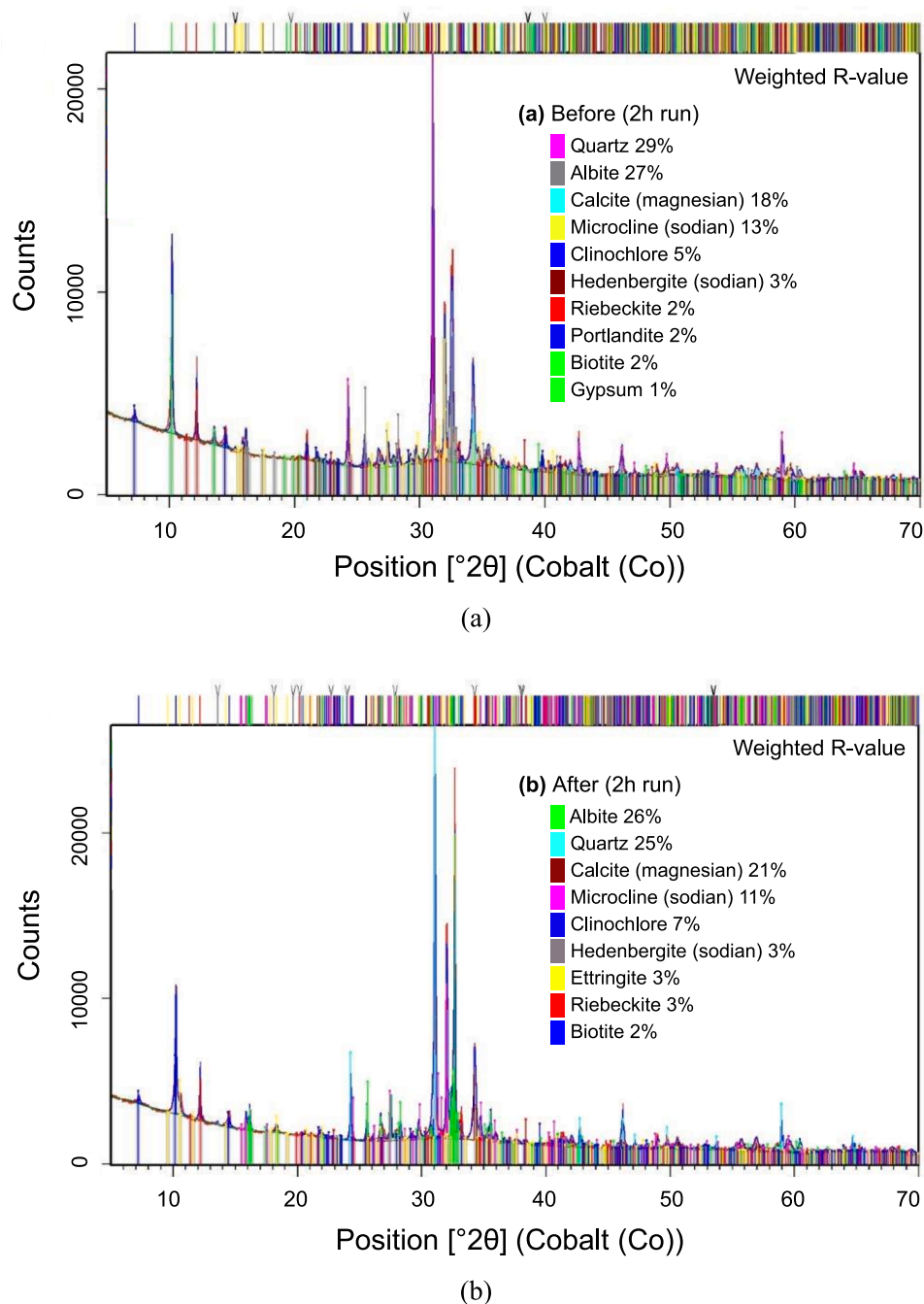


Fig. 7. X-ray diffraction (XRD) pattern for the RCA (a) before and (b) after sulfate adsorption. The absolute error is 3%, run for 2 h.

contact time. Therefore, for the rest of the experiments the contact time was set to 72 h.

Results of grain size analyses, are presented in Fig. 13. Clearly, the optimal size is identified as  $< 80 \mu\text{m}$  for the adsorption process. The trend shows that smaller particles result in a higher adsorption due to the availability of a higher surface area and adsorptive sites. Generally, coarser grain sizes may be suitable for filter-type applications while finer sizes are more suited for stirred reactors.

Carbonate minerals neutralize the acidic water; in lower pH values, the percentage of sulfate removal increased. As explained by the pH (pzc) study, RCA surface is positively charged in low pH conditions, which results in higher adsorption of sulfate anions due to the electrostatic attraction. Fig. 14 shows that the highest sulfate removal percentage (85%) was obtained at pH equal to 2, in contrast to the pH value

of 12 that resulted in the lowest sulfate removal (33%). Generally, also oxyanions are adsorbed at lower pH values more effectively (Kozyatnyk, 2016).

At lower pH values, the sulfate ions are more likely to be attracted to the predominantly positively charged sites on the surface of the adsorbent material, resulting in a higher rate of adsorption. Sulfate ions are also more stable at lower pH levels and available for adsorption. The electrostatic attraction also is stronger at lower pH levels, as the negative charge of the ion is more concentrated. This allows the ion to bind more strongly to the crystal surface, resulting in increased metal adsorption.

### 3.3. Metals removal testing

A set of lower doses of RCA was assessed for iron removal. It was

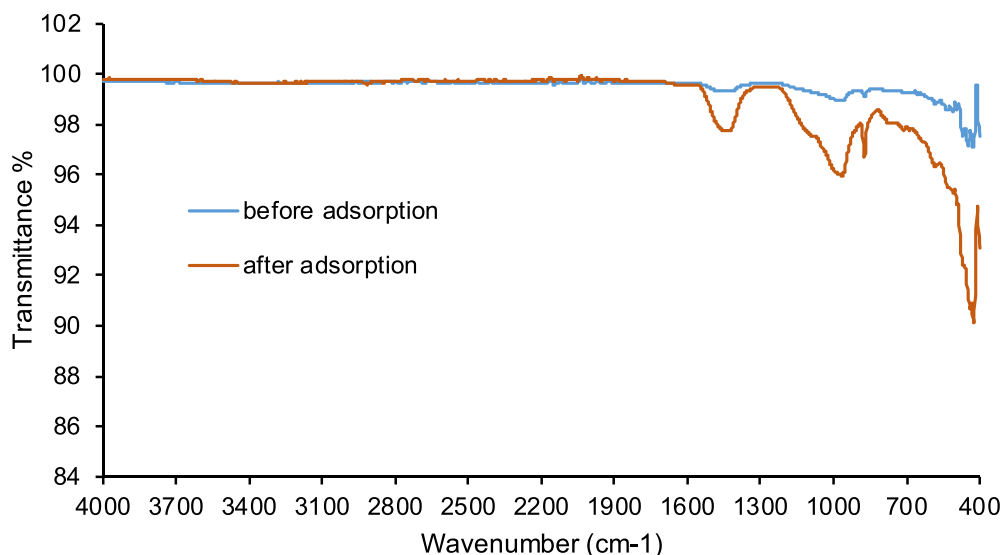


Fig. 8. Fourier Transform Infrared Spectroscopy (FT-IR) spectra of RCA before and after sulfate adsorption.

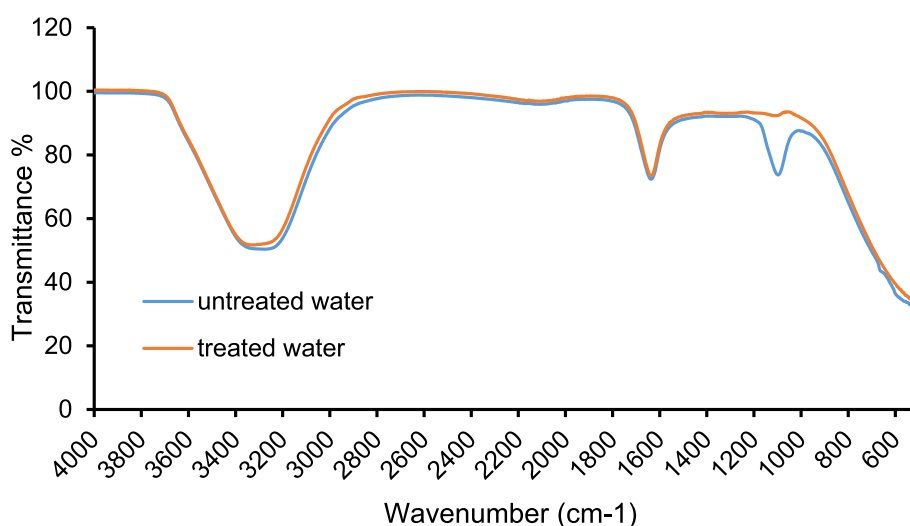


Fig. 9. Fourier Transform Infrared Spectroscopy (FT-IR) spectra of the solid content of the water samples before and after sulfate adsorption.

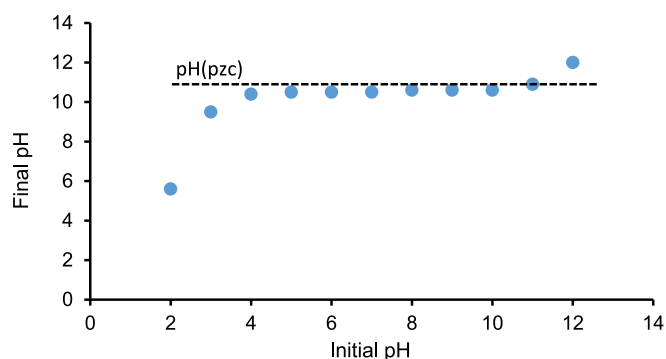


Fig. 10. Ph(pzc) measurement. experimental conditions: sorbent dose: 0.05 g, background electrolyte: 25 mL 0.1 M NaCl solution, contact time 24 h.

observed that iron is removed efficiently and quickly within < 30 min of contact time, with a very small amount of the adsorbent dose, shown in Fig. 15. It is also observed that the pH value in Aijala AMD water increased from the initial pH value of 4 to 7 in < 30 min. Iron removal

can be identified by both adsorption and precipitation.

The removal or release of metals was examined with X-ray fluorescence spectroscopic analyses of the water phase before and after the tests. The results of metal reaction after adsorption experiments by adsorbent dosage in the range of 0.05 to 5 g/L are tabulated in Fig. 16. Manganese (Mn: 94–96 %), copper Cu: (61–72 %), zinc (Zn: 96–97%), and lead (Pb: 75–77%) were removed by increasing the adsorbent dosage. Some degrees of metal release were also observed, as presented in Table 5. High amounts of calcium (Ca: 121.9 mg/L) and potassium (K: 9.15 mg/L) were released to the treated water with adsorbent dose of 1 g/L of as previously witnessed by the EDS outcomes presented in Fig. 6. Some levels of strontium (Sr: 0.44 mg/L), chromium (Cr: 0.035 mg/L), and cobalt (Co: 0.02 mg/L) were also released after adsorption treatment, yet the concentrations of these released unwanted metals were very low and below their environmental standard levels. However, the releases of metals increased with increasing adsorbent dosage. Therefore, the use of even higher dosages may result in higher concentrations of released metals, a feature that should be considered in eventual applications. Sr typically replaces Ca in minerals, and cement (e.g., the cement used here) typically contains some chromium. However, the concentration of Cr in cement is usually decreased before selling to avoid

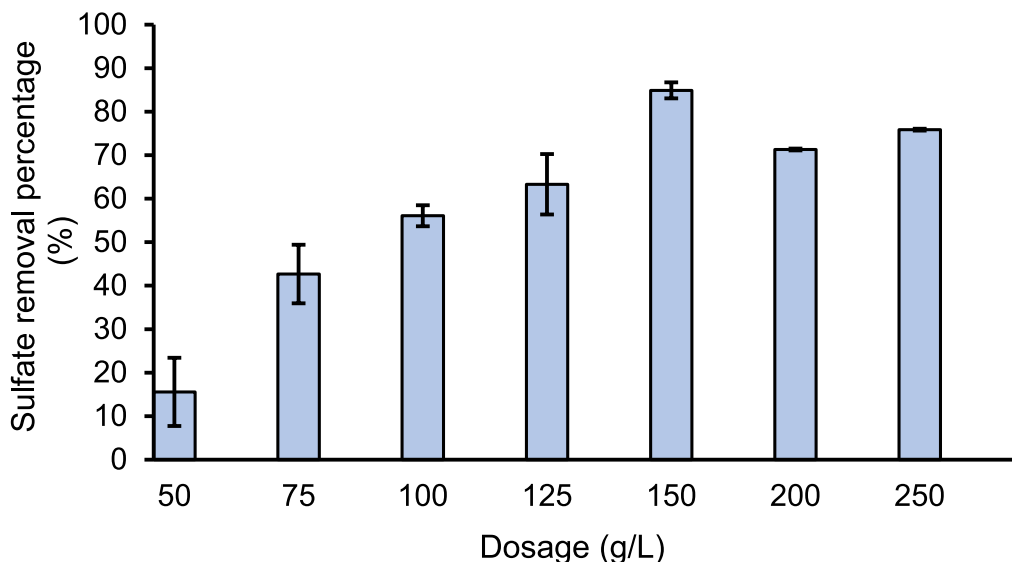


Fig. 11. Effect of sorbent dosage on sulfate removal (%); Experimental conditions: time 72 h, pH adjusted at 2, 210 rpm, size < 80 μm.

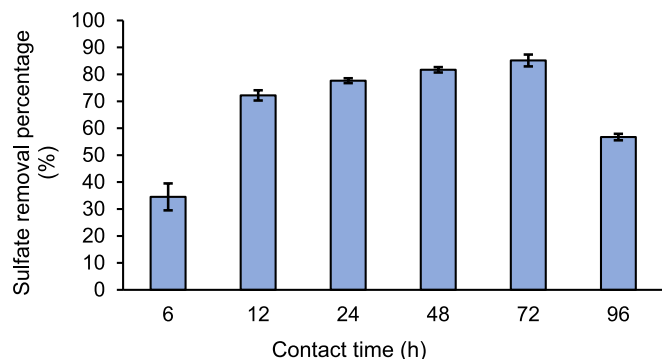


Fig. 12. Effect of adsorption contact time on sulfate removal (%). Experimental conditions: dose 150 g/L, Aijala AMD, pH adjusted at 2, 210 rpm, particle size < 80 μm.

health hazards. The concentration of Cr after trace metal adsorption with the highest dosage was measured as 0.053 mg/L, which is at the standard level suggested by WHO (Table 5) and 0.03 mg/L more than in

the original water.

By comparing the removed and released metals in Fig. 16 and Table 5, it can be concluded that the dosage of 1 g/L, with a size of < 80 μm of RCA, has the optimal results in neutralized pH value, with more efficient metal removal and less releasing elements.

#### 4. Conclusions

This research introduced RCA as a sustainable and locally available material for AMD treatment. The RCA material was thoroughly examined before and after water treatment using standard characterization methods including BET, SEM-EDS, elemental mapping, as well as XRD and FT-IR. The characterization revealed that the treatment was effective and the pollutants such as sulfate and metals were removed from water to the spent RCA. Experimental adsorption processes were conducted for Aijala AMD water treatment using RCA. Batch method was applied for all experiments. The effects of various parameters including adsorbent dosage, contact time, particle size, and pH on the adsorption process were examined for sulfate removal.

The more available active sites provided by larger RCA mass increased the sulfate ions removal. The highest sulfate removal was achieved at the contact time of 72 h. The optimal particle size of RCA

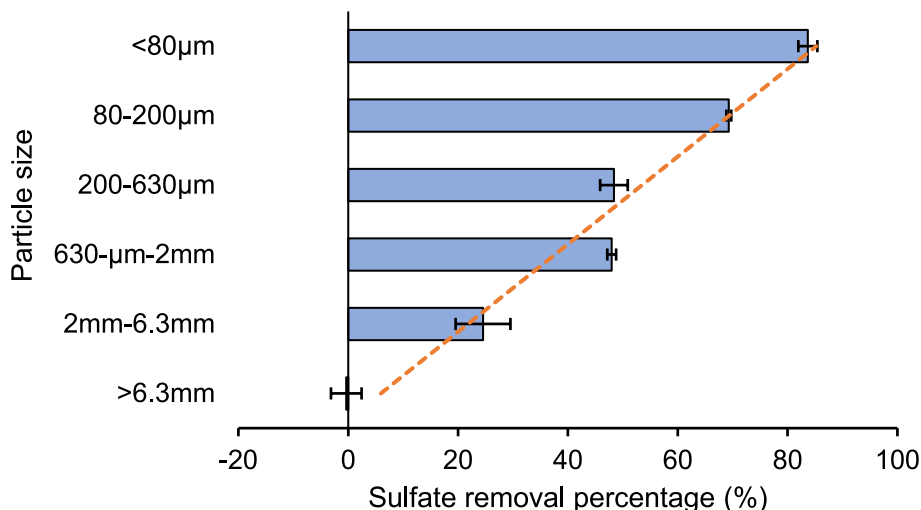


Fig. 13. Effect of RCA particle size on sulfate removal (%); Experimental conditions: dose 150 g/L, contact time 72 h, Aijala AMD, pH adjusted at 2, 210 rpm.

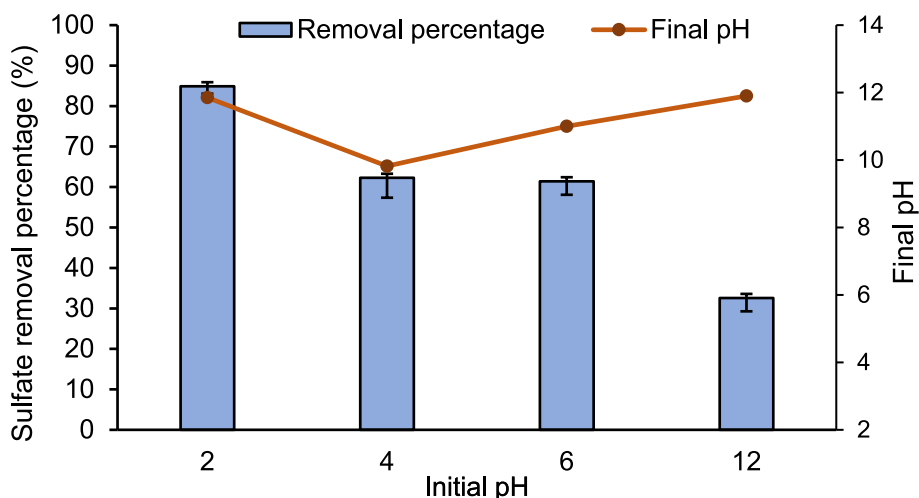


Fig. 14. Effect of pH on the sulfate adsorption onto the RCA; Experimental conditions: dose 150 g/L, contact time 72 h, Aijala AMD, size < 80 μm, 210 rpm.

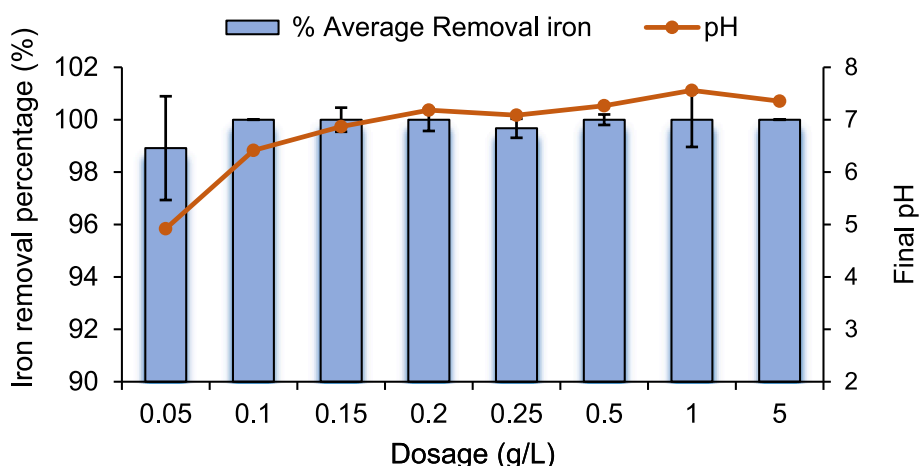


Fig. 15. Effect of sorbent dosage on iron removal (%); Experimental conditions: time 24 h, 210 rpm, size < 80 μm.

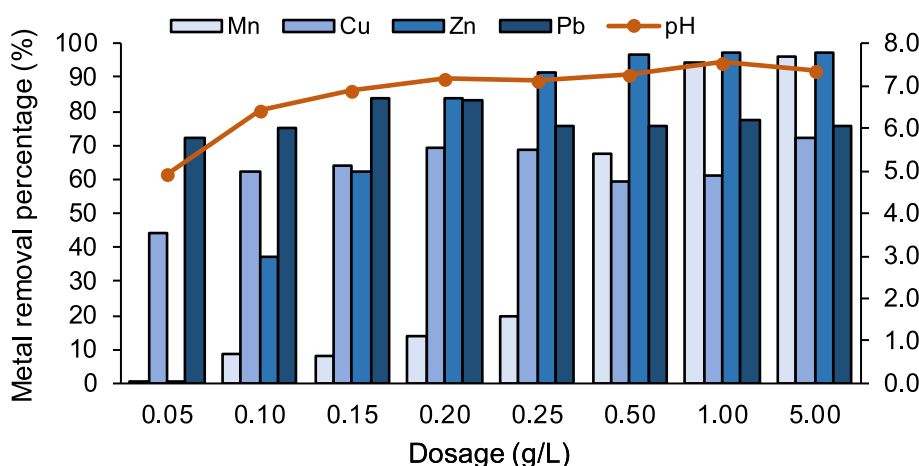


Fig. 16. Effect of sorbent dosage on heavy metal removal (%); Experimental conditions: time 24 h, 210 rpm, size < 80 μm, no pH adjustments.

was identified as < 80 μm for a higher adsorption of the metals and sulfate. The highest sulfate removal percentage was obtained at the pH value of 2. The pH value in Aijala AMD water was increased from the initial pH equal to 4 to a neutral pH by adding small quantities of RCA.

Furthermore, the adsorption of metals including iron, zinc,

manganese, copper, and lead were studied. Iron ions were removed efficiently, and quickly, within < 30 min of contact time, with a very small dose of the adsorbent. The results for metal adsorption, by adsorbent dosage in the range of 0.05 to 5 g/L, showed that manganese (Mn: 94–96 %), copper (Cu: 61–72 %), zinc (Zn: 96–97%), and lead (Pb:

Table 5

Releasing metals during the adsorption process.

Dosage (g/L)	pH	Metal released concentration (mg/L)				
		Ca	K	Sr	Cr	Co
Standard level (WHO, 1996)	6.5–8.5	75–200	10–50	7	0.05	0.05–1
Original water (Aijala)	4	102	6.84	0.38	0.02	0.01
0.05	4.9	101.1	6.86	0.40	0.03	0.03
0.10	6.4	94.5	6.34	0.38	0.03	0.02
0.15	6.9	105.7	6.90	0.41	0.03	0.029
0.20	7.2	105	6.99	0.40	0.027	0.02
0.25	7.1	112	7.57	0.42	0.027	0.02
0.50	7.3	114	8.34	0.43	0.018	0.017
1	7.5	121.9	9.15	0.44	0.035	0.02
5	7.4	233	19.48	0.75	0.053	0.018

Note: Sr concentration provided based on Canadian Guideline Technical Document, 7.0 mg/L is suggested as maximum concentration in drinking water (HealthCanada, 2018).

75–77%) were removed effectively. Heavy metal measurements also revealed that the adsorption process releases calcium and potassium, while consuming sulfur, oxygen, iron, and aluminum from AMD.

Accordingly, the removal of sulfate from low-pH mine water can be optimized by implementing a filtration system that allows for the pH to increase after sulfate removal, as low pH favors sulfate removal while high pH favors metal precipitation. The physical processes can be used to increase the pH of the water.

The results presented in this research demonstrate that using recycled concrete materials are a promising sustainable and passive method for acid mine drainage treatment. Herein, the consideration is on the low-cost and locally availability of waste and natural materials compared to the higher efficiency, yet expensiveness of engineered materials such as activated carbon. Also, economic and life cycle assessment can be considered for future studies. Although this paper deals with the study of heavy metal and sulfate removal from AMD, due to the lack of physical properties and ICP measurements of the sludge, still a long-term investigation with special emphasis on how RCA behaves after the treatment as part of the passive system is required.

### Declaration of Competing Interest

The authors declare that they have no known competing financial interests or personal relationships that could have appeared to influence the work reported in this paper.

### Data availability

No data was used for the research described in the article.

### Acknowledgments

This research was funded by the Maa- ja Vesitekniiikan Tuki, Helsinki, Finland.

The authors would like to acknowledge the assistance of Aino Pelto, Marina Sushko, and Heikki Särkkä in the laboratory work, of Abdelaziz Ramzy with the SEM-EDS measurements, of Akseli Torppa with the XRD measurements, of Benjamin Wilson for giving access to the facilities provided by the Academy of Finland's RawMatTERS Finland Infrastructure (RAMI-FIRI) program, of Afsoun Farzan in FT-IR analysis, of Jani Pieksemä for providing the material, and of Arto Pullinen in collecting samples from the site. Advisory support from Roza Yazdani and Sami Häkkinen is appreciated.

### Appendix A. Supplementary data

Supplementary data to this article can be found online at <https://doi.org/10.1016/j.clema.2023.100205>.

[org/10.1016/j.clema.2023.100205](https://doi.org/10.1016/j.clema.2023.100205).

### References

- Aguiar, A.O., Andrade, L.H., Ricci, B.C., Pires, W.L., Miranda, G.A., Amaral, M.C.S., 2016. Gold acid mine drainage treatment by membrane separation processes: An evaluation of the main operational conditions. *Separation and Purification Technology* 170, 360–369. <https://doi.org/10.1016/j.seppur.2016.07.003>.
- Ali, I., Gupta, V.K., 2007. Advances in water treatment by adsorption technology. *Nature Protocols* 1 (6), 2661–2667. <https://doi.org/10.1038/nprot.2006.370>.
- Alley, E. R., 2007. *Water Quality Control Handbook*. In Environment (Vol. 1). <https://doi.org/10.1036/0071467602>.
- Arroyo, Y.R.R., Siebe, C., 2007. Weathering of sulphide minerals and trace element speciation in tailings of various ages in the Guanajuato mining district. Mexico. *Catena* 71 (3), 497–506. <https://doi.org/10.1016/j.catena.2007.03.014>.
- Bakatula, E.N., Richard, D., Neculita, C.M., Zagury, G.J., 2018. Determination of point of zero charge of natural organic materials. *Environmental Science and Pollution Research* 25 (8), 7823–7833. <https://doi.org/10.1007/s11356-017-1115-7>.
- Baruah, B.P., Khare, P., 2010. Mobility of trace and potentially harmful elements in the environment from high sulfur Indian coal mines | Elsevier Enhanced Reader. *Applied Geochemistry*. <https://reader.elsevier.com/reader/sd/pii/S088329271000185X?token=1BB5B6CB36D3C70BF76383575413E58B7546711CBF1938FB580344E84B113707C5205FCDE317FD3A1E030CD0A1DB1BED>.
- Carrero, S., Pérez-López, R., Fernandez-Martinez, A., Cruz-Hernández, P., Ayora, C., Poulain, A., 2015. The potential role of aluminium hydroxysulphates in the removal of contaminants in acid mine drainage. *Chemical Geology* 417, 414–423. <https://doi.org/10.1016/j.chemgeo.2015.10.020>.
- Fernando, W.A.M., Ilnkoon, I.M.S.K., Syed, T.H., Yellishetty, M., 2018. Challenges and opportunities in the removal of sulphate ions in contaminated mine water: A review. In: *Minerals Engineering*, Vol. 117. Elsevier Ltd., pp. 74–90. <https://doi.org/10.1016/j.mineng.2017.12.004>.
- Galhardi, J.A., Bonotto, D.M., 2016. Hydrogeochemical features of surface water and groundwater contaminated with acid mine drainage (AMD) in coal mining areas: a case study in southern Brazil. *Environmental Science and Pollution Research* 23 (18), 18911–18927. <https://doi.org/10.1007/s11356-016-7077-3>.
- Grande, J.A., de la Torre, M.L., Cerón, J.C., Beltrán, R., Gómez, T., 2010. Overall hydrochemical characterization of the Iberian Pyrite Belt. Main acid mine drainage-generating sources (Huelva, SW Spain). *Journal of Hydrology* 390 (3–4), 123–130. <https://doi.org/10.1016/j.jhydrol.2010.06.001>.
- Hammack, R.W., Edenborn, H.M., Dvorak, D.H., 1994. Treatment of water from an open-pit copper mine using biogenic sulfide and limestone: A feasibility study. *Water Research* 28 (11), 2321–2329. [https://doi.org/10.1016/0043-1354\(94\)90047-7](https://doi.org/10.1016/0043-1354(94)90047-7).
- Hase, T., 1999. *Organic spectrometry* (8th ed., pp. 20–39).
- HealthCanada. (2018). *Strontium in Drinking Water - Guideline Technical Document for Public Consultation - Canada.ca*. Federal-Provincial-Territorial Committee on Drinking Water. <https://www.canada.ca/en/health-canada/programs/consultation-strontium-drinking-water/document.html>.
- Ho, H.J., Iizuka, A., Vadapalli, V.R.K., Coetzee, H., Petrik, L., Petersen, J., Ojumu, T., 2023. Potential investigation of concrete fines as an alternative material: A novel neutralizer for acid mine drainage treatment. *Environmental Technology & Innovation* 29, 102985. <https://doi.org/10.1016/J.ETI.2022.102985>.
- Iakovleva, E., Mäkilä, E., Salonen, J., Sitarz, M., Sillanpää, M., 2015. Industrial products and wastes as adsorbents for sulphate and chloride removal from synthetic alkaline solution and mine process water. *Chemical Engineering Journal* 259, 364–371. <https://doi.org/10.1016/j.cej.2014.07.091>.
- Iizuka, A., Ho, H.J., Sasaki, T., Yoshida, H., Hayakawa, Y., Yamasaki, A., 2022. Comparative study of acid mine drainage neutralization by calcium hydroxide and concrete sludge-derived material. *Minerals Engineering* 188, 107819. <https://doi.org/10.1016/J.MINENG.2022.107819>.
- Isomäki, O.-P., 1990. The sulphid ore deposits in the Orijärvi-Ajala field 0111-Pekka Isomäki Outokumpu Oy.
- Johnson, D.B., Hallberg, K.B., 2005. Acid mine drainage remediation options: a review. *Science of The Total Environment* 338 (1–2), 3–14. <https://doi.org/10.1016/J.SCITOTENV.2004.09.002>.
- Kefeni, K.K., Msagati, T.A.M., Mamba, B.B., 2017. Acid mine drainage: Prevention, treatment options, and resource recovery: A review. *Journal of Cleaner Production* 151, 475–493. <https://doi.org/10.1016/j.jclepro.2017.03.082>.
- Keng, P.S., Lee, S.L., Ha, S.T., Hung, Y.T., Ong, S.T., 2014. Removal of hazardous heavy metals from aqueous environment by low-cost adsorption materials. *Environmental Chemistry Letters* 12 (1), 15–25. <https://doi.org/10.1007/s10311-013-0427-1>.
- Kokkola, M., 1982. Jätealueen soijattutkimus Kisko, Aijala.
- Komnitsas, K., Bartzas, G., Paspaliaris, I., 2004. Efficiency of limestone and red mud barriers: Laboratory column studies. *Minerals Engineering* 17 (2), 183–194. <https://doi.org/10.1016/j.mineng.2003.11.006>.
- Kozyatnyk, I., 2016. *Filtration Materials for Groundwater: A Guide to Good Practice*. IWA Publishing.
- Kumara, G. M. P., Saito, T., Asamoto, S., & Kawamoto, K., 2017. Review the applicability of construction and demolition waste as low-cost adsorbents to remove heavy metals in wastewater. <https://doi.org/10.21660/2018.42.7148>.
- Lakherwal, D., 2014. Adsorption of Heavy Metals: A Review. In *International Journal of Environmental Research and Development* Vol. 4(1), 41–48. <http://www.ripublication.com/ijerd.htm>.
- Lim, A.P., Aris, A.Z., 2014. A review on economically adsorbents on heavy metals removal in water and wastewater. *Reviews in Environmental Science and Biotechnology* 13 (2), 163–181. <https://doi.org/10.1007/s11157-013-9330-2>.

- Lin, S.-H., Juang, R.-S., 2009. Adsorption of phenol and its derivatives from water using synthetic resins and low-cost natural adsorbents: A review. *Journal of Environmental Management* 90 (3), 1336–1349.
- Macías, F., Pérez-López, R., Caraballo, M.A., Cánovas, C.R., Nieto, J.M., 2017. Management strategies and valorization for waste sludge from active treatment of extremely metal-polluted acid mine drainage: A contribution for sustainable mining. *Journal of Cleaner Production* 141, 1057–1066. <https://doi.org/10.1016/j.jclepro.2016.09.181>.
- Masukume, M., Onyango, M.S., Maree, J.P., 2014. Sea shell derived adsorbent and its potential for treating acid mine drainage. *International Journal of Mineral Processing* 133, 52–59. <https://doi.org/10.1016/j.minpro.2014.09.005>.
- Menegaki, M., Damigos, D., 2018. A review on current situation and challenges of construction and demolition waste management. *Current Opinion in Green and Sustainable Chemistry* 13, 8–15.
- Mohan, S., Gandhimathi, R., 2009. Removal of heavy metal ions from municipal solid waste leachate using coal fly ash as an adsorbent. *Journal of Hazardous Materials* 169 (1–3), 351–359. <https://doi.org/10.1016/j.jhazmat.2009.03.104>.
- Nedeljković, M., Visser, J., Šavija, B., Valcke, S., Schlangen, E., 2021. Use of fine recycled concrete aggregates in concrete: A critical review. *Journal of Building Engineering* 38, 102196.
- Oates, J.A.H., 1998. *Lime and Limestone: Chemistry and Technology*. Wiley, Production and Uses.
- Pacheco-Torgal, F., Lourenco, P.B., Labrincha, J.A., Kumar, S., Chindaprasirt, P., 2015. *Eco-efficient Masonry Bricks and Blocks: Design, Properties and Durability* - Google Books. Woodhead publishing, Elsevier, pp. 191–226.
- Pallewatta, S., Weerasooriyagedara, M., Bordoloi, S., Sarmah, A.K., Vithanage, M., 2023. Reprocessed construction and demolition waste as an adsorbent: An appraisal. *Science of The Total Environment* 882, 163340. <https://doi.org/10.1016/j.scitotenv.2023.163340>.
- Panda, L., Jena, S.K., Rath, S.S., Misra, P.K., 2020. Heavy metal removal from water by adsorption using a low-cost geopolymer. *Environmental Science and Pollution Research* 27 (19), 24284–24298. <https://doi.org/10.1007/s11356-020-08482-0>.
- Potgieter-Vermaak, S.S., Potgieter, J.H., Monama, P., van Grieken, R., 2006. Comparison of limestone, dolomite and fly ash as pre-treatment agents for acid mine drainage. *Minerals Engineering* 19 (5), 454–462. <https://doi.org/10.1016/j.mineng.2005.07.009>.
- Purchase, C.K., Al Zulayq, D.M., O'Brien, B.T., Kowalewski, M.J., Berenjian, A., Tarighaleslami, A.H., Seifan, M., 2022. Circular Economy of Construction and Demolition Waste. A Literature Review on Lessons, Challenges, and Benefits. *Materials (Basel)* 15(1):76. 15 (1), 76.
- Qureshi, A., Maurice, C., Öhlander, B., 2016. Potential of coal mine waste rock for generating acid mine drainage. *Journal of Geochemical Exploration* 160, 44–54. <https://doi.org/10.1016/j.gexplo.2015.10.014>.
- Rafatullah, M., Sulaiman, O., Hashim, R., Ahmad, A., 2010. Adsorption of methylene blue on low-cost adsorbents: A review. *Journal of Hazardous Materials* 177 (1–3), 70–80.
- Roedder, E., 1959. *Problems in the Disposal of Acid Aluminum Nitrate High-level Radioactive Waste Solutions by Injection Into Deep-lying Permeable Formations*. Government Printing Office, U.S.
- Rudus., 2019. Rudus. Rudus. <https://www.rudus.fi/>.
- Shim, M.J., Choi, B.Y., Lee, G., Hwang, Y.H., Yang, J.S., O'Loughlin, E.J., Kwon, M.J., 2015. Water quality changes in acid mine drainage streams in Gangneung, Korea, 10years after treatment with limestone. *Journal of Geochemical Exploration* 159, 234–242. <https://doi.org/10.1016/j.gexplo.2015.09.015>.
- Silva, A.M., Lima, R.M.F., Leão, V.A., 2012. Mine water treatment with limestone for sulfate removal. *Journal of Hazardous Materials* 221–222, 45–55. <https://doi.org/10.1016/j.jhazmat.2012.03.066>.
- Sipilä, P., 1994. Aijalan, pyhasalmen ja makolan sulfidimikroavosten rikastamoiden jatealueiden ymp aristovaikutukset.
- Socrates, G., 2002. Infrared and Raman Characteristic Group Frequencies. *Journal of the American Chemical Society*, 124(8), 1830–1830. <https://doi.org/10.1021/ja0153520>.
- Szlachta, M., Neitola, R., Peräniemi, S., Vepsäläinen, J., 2020. Effective separation of uranium from mine process effluents using chitosan as a recyclable natural adsorbent. *Separation and Purification Technology* 253 (April), 1–11. <https://doi.org/10.1016/j.seppur.2020.117493>.
- Valjus, T., Huotari, T., Lerssi, J., Markovaara-Koivisto, M., Tarvainen, T., 2017. Geophysical Study of a Potential Source of Secondary Raw Materials - The Aijala Mine Tailings Area Southern Finland. <https://doi.org/10.3997/2214-4609.201702124>.
- Wang, F.Y., Wang, H., Ma, J.W., 2010. Adsorption of cadmium (II) ions from aqueous solution by a new low-cost adsorbent-Bamboo charcoal. *Journal of Hazardous Materials* 177 (1–3), 300–306. <https://doi.org/10.1016/j.jhazmat.2009.12.032>.
- WHO., 2011. Background document for development of WHO Guidelines for Drinking-water Quality. In World Health Organization.
- WHO., 1996. Guidelines for drinking-water quality. World Health Organization & International Programme on Chemical Safety, 2, 973.
- WHO., 2008. Guidelines for drinking-water quality.
- Yazdani, M. R., Duimovich, N., Tiraferri, A., Laurell, P., Borghei, M., Zimmerman, J. B., Vahala, R., 2019. Tailored mesoporous biochar sorbents from pinecone biomass for the adsorption of natural organic matter from lake water. *Journal of Molecular Liquids*, 291.
- Yazdani, M.R., Tuutijärvi, T., Bhatnagar, A., Vahala, R., 2016. Adsorptive removal of arsenic(V) from aqueous phase by feldspars: Kinetics, mechanism, and thermodynamic aspects of adsorption. *Journal of Molecular Liquids* 214, 149–156. <https://doi.org/10.1016/j.molliq.2015.12.002>.
- Younger, P. L., Banwart, S. A., & Hedin, R. S., 2002. *Mine Water: Hydrology, Pollution, Remediation*. Kluwer Academic Publishers. <https://doi.org/10.1007/978-94-010-0610-1>.